Vortex Interactions and Decay in Aircraft Wakes

Alan J. Bilanin,* Milton E. Teske,† and Guy G. Williamson‡
Aeronautical Research Associates of Princeton, Inc., Princeton, N.J.

The dynamic interactions of aircraft wake vortices are investigated using both inviscid and viscous models. The phenomenon of vortex merging resulting in the rapid aging of a vortex wake is examined in detail. It is shown that the redistribution of vorticity from convection and diffusion during merging is a mechanism effective in reducing the hazard of a wake. Inviscid computations show that the merging phenomenon may be sensitive to small changes in spanwise load distribution and that the fuselage vortex shed from the wing-fuselage junction can play a significant role in promoting merging of wing tip and flap vortices. Vortex wake merging computations using a second-order closure model of turbulent transport indicate that a low hazard wake occurs when the generating aircraft trails flap and wing tip vortices of the same strength and sign. This optimum is achieved when the flap vortex is located outboard approximately 40% of the distance to the tip vortex.

Nomenclature

A	= aspect ratio
c	= local chord
c_{ℓ_α}	= sectional lift coefficient
C_{ℓ}	= rolling moment coefficient
C_L	= lift coefficient
d	= separation distance between vortices
e	= half-length of a circulation contour box
P	= pressure
q	= rms of twice the turbulent kinetic energy
r	= radius
r_c	= viscous core radius or variance
s	= wing semispan
t	= time
u_i	= turbulent velocity component in the ith direction
$U_i = (U, V, W)$	= velocity components in the x,y,z system
U_∞	= freestream velocity
$x_i = (x,y,z)$	= Cartesian coordinates
$\bar{y}$	= centroid of trailed vorticity
Γ	= circulation
Δ	= vertical point vortex separation
ϵ	= turbulent dissipation rate
ζ	= streamwise component of vorticity
Λ	= macroscale or integral scale parameter
ν	= kinematic viscosity
ρ	= density
ψ	= stream function
Subscripts	
f	= follower or flap
j	= wing-fuselage junction
max	= maximum
t	= tip
$< >$	= denotes ensemble average

I. Introduction

LOW hazard aircraft vortex wakes are produced when the configuration of an aircraft is such that multiple vortices are trailed which interact strongly enough to result in merging.[1-3] This phenomenon involves the convective and turbulent redistribution of trailed vorticity,[4-5] and is decidedly nonlinear. The development and operation of larger commercial aircraft favor a careful study of the merging process and the mechanisms involved in triggering it. There is now a need to understand viscous interactions in a vortex wake more fully. This paper examines the methods currently available to investigate vortex wakes and describes a new technique developed to predict the viscous interactions in a wake. This technique makes use of a computer code which solves the fluid equations of motion including turbulent transport through a second-order turbulent closure model of the Reynolds stress equations.

It seems appropriate to introduce the merging concept at this point in order that the reader may initially see the significance of the phenomenon. For that we consider the wake of an aircraft in its cruise and landing/takeoff configurations as illustrated in Fig. 1. The trailed vorticity of the cruise wake is found in two regions with distributions nearly axisymmetric (the left half of Fig. 1). The production of turbulence and the subsequent diffusion of vorticity across the nearly axisymmetric streamlines are suppressed by the centrifugal effect of the swirling velocity within each vortex.[6] Aging in the absence of atmospheric turbulence, wind shear, or stratification results only from modest amounts of turbulence generated in the vortices themselves (their distributions slowly diffuse from $t=0$ to $t=t_2$).

When an aircraft is in its landing or takeoff configuration, however, trailed multiple vortices form a wake,[7,8] similar to the one illustrated on the right half of Fig. 1. These vortices are both convected and strained by one another. This induced straining field is responsible for the merging or pairing of the vortices, which then results (by $t=t_1$ in Fig. 1) in the production of turbulence and an even wider (and faster) redistribution of the trailed vorticity. At comparable times after aircraft passage, the multiple-vortex wake has both a more widely spread distribution of vorticity as well as a spread rate which is greater than the wake from an aircraft in cruise configuration. If circulation in the half-plane is taken as a measure of the strength of the wake, no reduction in the circulation can occur until the trailed vorticity has diffused to the wake centerline (here shown at $t=t_2$). Turbulence produced during merging provides one mechanism for this diffusion. In fact, viscous interactions in an aircraft wake cannot be ignored if there is to be any attempt to predict the decay of wake intensity with distance downstream of the aircraft.

While this paper treats both inviscid and viscous techniques, our emphasis is on transport phenomena. The inviscid merging phenomenon has been investigated using distributions of point vortices by Rossow.[5] In Sec. II, we describe several inviscid techniques used to compute wake structure and vortex-vortex interaction. In Sec. III, we review

Received July 2, 1976; revision received Oct. 19, 1976.
Index categories: Jets, Wakes, and Viscid-Inviscid Flow Interactions; Viscous Nonboundary-Layer Flows.
*Senior Consultant. Member AIAA.
†Consultant.
‡Consultant. Member AIAA.

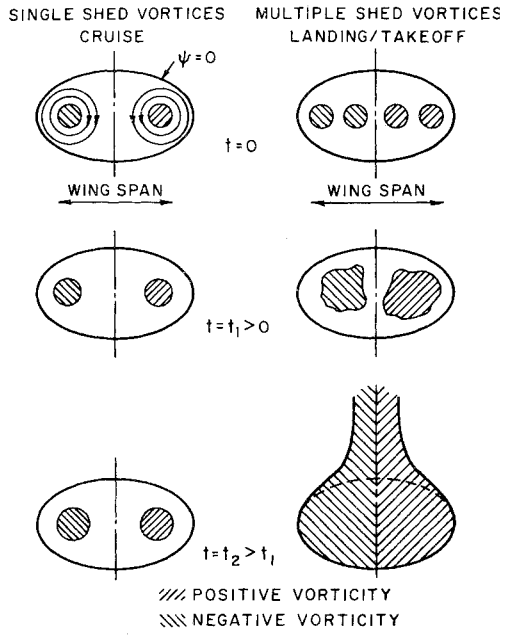

Fig. 1 Schematic representation of the merging process behind an aircraft in cruise and landing/takeoff. The solid single curves are the $\psi = 0$ streamlines in a frame of reference moving with the appropriate downwash velocity.

the turbulent model based on a second-order closure of the Reynolds stress equations, and briefly describe the computer code used to solve the model equations. In Sec. IV, we present a variety of vortex wake interaction problems,§ and determine what should prove to be a configuration for a low hazard vortex wake. Conclusions are offered in Sec. V.

II. Inviscid Description of Aircraft Wakes

While a mathematical model of an aircraft wake must include turbulent transport if there is to be any attempt to predict aging of the wake, considerable insight into wake structure and dynamics has been obtained from an inviscid description. Two inviscid techniques used to predict wake geometry and structure are briefly described here in an effort to obtain information regarding vortex merging as well as point out predictive limitations of these techniques. In particular, point vortex computations show that vortex merging may be sensitive to small changes in the wing lift distributions.

Method of Betz and Extensions

The method of Betz[9] relates the load distribution on a simply loaded wing to two axisymmetric distributions of swirling velocity in the distant rolled-up wake. This method is based on the application of certain integral "invariants" of a two-dimensional distribution of vorticity in a physically motivated manner. Many investigators have re-examined the Betz procedure and have extended the technique to include multiple vortices as well as distributed wing drag. These extensions have been recently reviewed in Ref. 6.

The comparison of measured swirl velocity distributions in the wakes of clean aircraft (cruise configuration) with distributions predicted by the Betz technique is remarkably good.[8] However, when an aircraft is in a dirty (landing or takeoff) configuration, the Betz technique predicts velocity distributions that depart significantly from those measured.[10] This discrepancy has been explained by the observations first made by Dunham[1] of the strong interaction and coalescing or merging of multiple vortices into a single, more diffuse vortex. The Betz method assumes *a priori* that each vortex trailed in the wake rolls up independently of the influence of other vortices present. The merging phenomenon is one in which the straining of vortex on vortex is the dominant interaction. Therefore, prediction by the Betz technique of the vortex velocity distributions in a multiple-vortex-pair wake, where vortices (particularly of like sign) come in close proximity, must necessarily fail. The Betz technique is a simple means of obtaining a first look at the structure of aircraft vortex wakes, but it cannot be used in situations where straining interactions between vortices are important.

Point Vortex Computations

The point vortex method computes the motion of a finite number of point vortices representing the vorticity trailed by a wing. Investigators have used this technique to simulate the roll-up of a sheet of vorticity trailed from the trailing edge of a wing, and the recent work of Fink and Soh[11] has shown how continuous rediscretization of a vortex sheet must be accomplished to minimize error. It is our intent here not to treat the details of roll-up of each vortex in a wake, but to study the trajectories of these vortices. The detailed roll-up problem may be found in Refs. 12-14.

Donaldson et al.[8] have given criteria to be followed to determine the number of vortices that will be trailed as the vortex wake of an aircraft. These criteria are applied to the wing lift distribution. The number of vortices that will roll up to form a wake equals the number of local maxima of the absolute value of the vortex sheet strength $|d\Gamma/dy|$. The trailed vortex sheet divides itself at local minima. Yates[15] has shown that these criteria are reasonable approximations under most situations. Exceptions occur when one vortex is of such weak strength that the tendency to roll up independently is dominated by the convective field of other vortices. These cases are not of interest here.

The procedure used here is to determine the strength and initial position of each vortex that will ultimately roll up and replace each vortex by one two-dimensional irrotational point vortex of equal strength. The subsequent motion of each point vortex is then computed. This procedure is appropriate insofar as only the position (centroid) of each discrete vortex is to be determined. The approximation of two-dimensionality is easily justified since the streamwise gradients in a vortex wake are the order of C_L/A.

Treating the vorticity as though it were concentrated at a point (centroid) is a concept whose justification rests with the fact that the motion of a vortex does not depend critically on the distribution of vorticity in the vortex. It may be shown[6] that the motion of the centroid of a two-dimensional distribution of vorticity is given by

$$\frac{d\bar{r}_c}{dt} = \frac{\int \bar{U}_0 \zeta dA}{\int \zeta dA} \tag{1}$$

where $\bar{U}_0$, is the velocity field induced by the presence of other distant distributions of vorticity, and ζ is the vorticity distribution of the vortex in question. The velocity of the centroid of vorticity is proportional to the irrotational velocities from the other discrete distributions of vorticity averaged with the vorticity over the area. The error in using a point vortex to represent the motion of the centroid of a distribution of vorticity is at worst of order $(a/d)^2$ where a is the characteristic dimension over which ζ is spread, and d is the distance to the nearest vortex.

§Since submission of the manuscript, Rossow[36] has presented a variety of multiple vortex merging studies using distributions of point vortices to represent continuous distributions of vorticity. The initial stages of merging which are dominated by convection compare quite favorably with the computations reported herein.

The horizontal and vertical velocities (V, W) of the centroid of each discrete vortex in a wake are then given by

$$V_j = \frac{dy_j}{dt} = -\frac{1}{2\pi}\sum_{i(i\neq j)}^{N}\frac{\Gamma_i(z_j - z_i)}{r_{ij}^2} + 0\left(\frac{a}{d}\right)^2 \tag{2a}$$

$$W_j = \frac{dz_j}{dt} = +\frac{1}{2\pi}\sum_{i(i\neq j)}^{N}\frac{\Gamma_i(y_j - y_i)}{r_{ij}^2} + 0\left(\frac{a}{d}\right)^2 \tag{2b}$$

for N vortices of individual strengths Γ_i located at (y_i, z_i); with $r_{ij}^2 = (y_j - y_i)^2 + (z_j - z_i)^2$. These equations may be programed and solved using standard techniques.

In the wake of an aircraft, some simplification occurs because the vortices exist only in pairs and are always located symmetrically about the aircraft centerline. Conservation of vertical fluid impulse requires that

$$J = \sum_{i}^{N}\Gamma_i y_i \tag{3}$$

remains constant throughout the ensuing vortex motion. As a result of the singularity at the center of each vortex, the kinetic energy of the fluid is infinite. It has been shown,[6] however, that the portion of the kinetic energy associated with the relative positions of the vortices is conserved and is given by

$$T = -\rho\pi\sum_{i}^{N}\sum_{\substack{j\\(i\neq j)}}^{N}\Gamma_j\Gamma_i \ln r_{ij} \tag{4}$$

proportional to the Kirchhoff-Routh path function.[16]

Initially confining our remarks to two-vortex-pair wakes, several observations about the nature of wake geometry can be made without resorting to the time-dependent solutions of Eqs. (2). If Δ is one-half the vertical separation between the two vortex pairs, Eq. (4) may be written

$$B\left((y_f/y_t)_0,\ (e/y_t)_0,\ \Gamma_f/\Gamma_t\right) = \frac{\Delta^2 + (y_t + y_f)^2}{\Delta^2 + (y_t - y_f)^2}\cdot\left(\frac{y_f}{y_t}\right)^{\Gamma_f/\Gamma_t} \tag{5}$$

Now Eqs. (3) and (5) contain all the information needed to determine all possible relative trajectories. At the wing, J and B can be evaluated with $\Delta = 0$. That is, the tip vortex of strength Γ_t is initially located at $(y_{t0}, 0)$ and the flap vortex of strength Γ_f is initially located at $(y_{f0}, 0)$. Equations (3) and (5) may now be examined to determine the values of B and J which have vortex trajectories that are unbounded $(\Delta \to \infty)$. These results are summarized in Fig. 2.

Two-vortex-pair wakes may be classified into one of four categories depending on whether the pairs are of the same or opposite sign, and whether they separate or remain together. Vortices of the same sign remaining together are most typical of conventional aircraft with one set of flaps deployed. The region on Fig. 2 for $\Gamma_f/\Gamma_t > 0$ denoted "remain together" is of most interest for vortex merging. The trajectories from two such time-dependent solutions of Eq. (2) are shown in Fig. 3, where the structure of vortex pairs that remain together and those that separate are illustrated.

Vortex wakes of full-scale aircraft, which may be represented by two-vortex-pair wakes and fall in the regions denoted "remain together" in Fig. 2, should be expected to merge at some distance behind the aircraft. This distance as well as the redistribution of vorticity which occurs as a result of merging can only be predicted from a model that includes transport. In a more realistic representation of an aircraft wing, the loss of lift at the wing-fuselage junction causes the shedding of a third vortex pair near the wing root. The inclusion of a third pair of vortices forces the numerical solution of Eq. (2). As an example of the insight that can

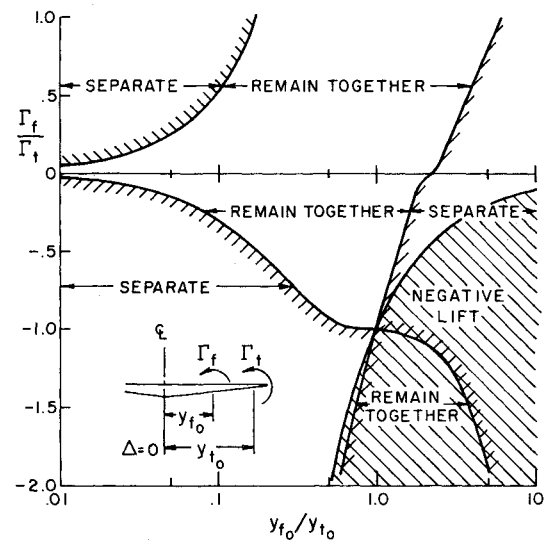

Fig. 2 Wake classification chart for two-vortex-pair wakes initialized as shown in the insert. y_{t0} is measured to the largest positive vortex.

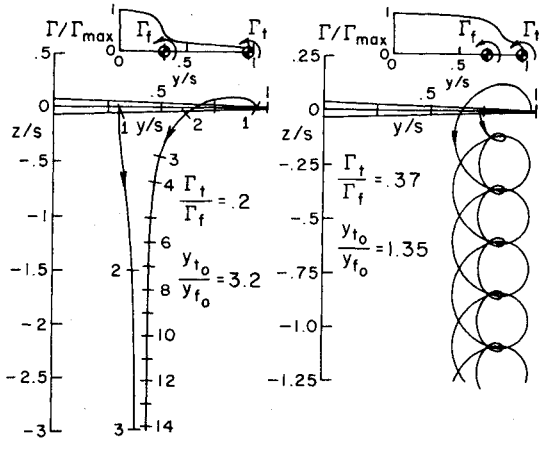

Fig. 3 Point vortex trajectory calculations for strong and weak interactions between Γ_t and Γ_f. In the weak (left) case the pair diverges as shown by the unit time marks on the trajectories themselves. In the strong (right) case the pairs remain together.

be obtained with point vortex computations, we now consider the computed lift distribution typical of the B-747 during landing as shown in Fig. 4 (Ciffone and Lonzo[7]). The Betz-Donaldson roll-up technique predicts the presence of three distinct vortices: at the tip ($\Gamma_t = 0.3\ \Gamma_f$), flap (Γ_f), and fuselage ($\Gamma_j = -0.7\ \Gamma_f$) positioned as shown at $y_t = 0.95s$, $y_f = 0.4s$ and $y_j = 0.125s$, respectively, where s is the wing semispan. In Ref. 7 flow visualization experiments in a towing tank show that merging between the tip and flap vortices over distances observed does not occur for this configuration. We may confirm this observation by solving Eq. (2) for the downstream locations of the three pairs.

In Fig. 5 we show this configuration ($\Gamma_j/\Gamma_f = -0.7$) and analyze the sensitivity of merging to a variation of the fuselage-to-flap ratio. Clearly, as the calculation proceeds downstream, the -0.7 curve shows that the distance between the tip and flap vortices increases monotonically over the distances computed. By decreasing the ratio Γ_j/Γ_f, the closest separation between the two vortices is reduced, until a point of minimum separation distance is reached with $\Gamma_j/\Gamma_f = -0.3$. However, a further reduction increases the separation distance. Since it is reasonable to presume that the proximity of tip and flap vortices can be directly correlated with the likelihood of merging (calculations in Sec. IV sub-

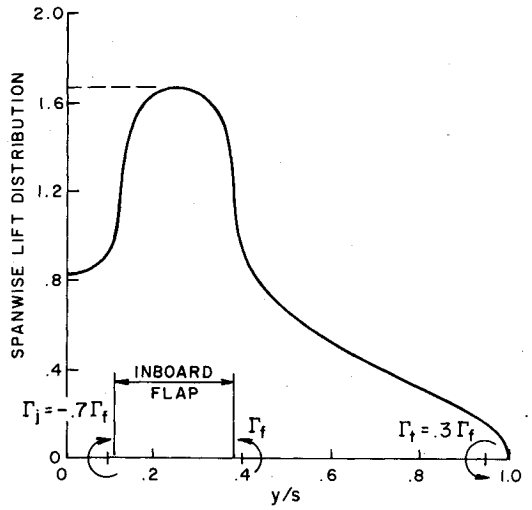

Fig. 4 Predicted spanwise lift distribution along a wing with total lift coefficient = 0.809 (Ref. 7) and the Betz roll-up representation into three distinct vortices at the tip, flap, and wing-fuselage junction.

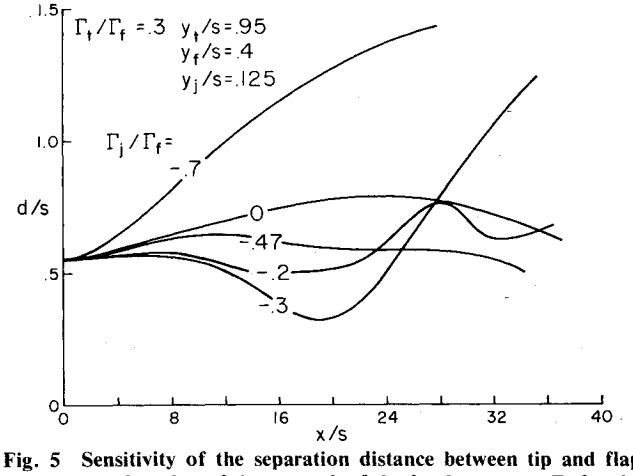

Fig. 5 Sensitivity of the separation distance between tip and flap vortices as a function of the strength of the fuselage vortex Γ_j for the load distribution on Fig. 4 with $A = 7$ and $C_L = 0.809$. Thus, $x/s = 25.0t\Gamma_f/2\pi s^2$.

stantiate this), it is not surprising that Ciffone and Lonzo did not observe merging for the configuration tested.

The sensitivity of distance between flap and tip vortices under change in the position of the fuselage vortex for the fixed strengths ratio $\Gamma_j/\Gamma_f = -0.47$ is shown in Fig. 6. The $y_j/s = 0.125$ reproduces the corresponding curve shown in Fig. 5. Also included are the $y_j/s = 0.0$ and 0.2 curves. In the latter case, the separation distance is reduced drastically (to 9% of the wing semispan), after which the two vortices separate rapidly. The question of whether merging occurs near the point of minimum separation must be investigated with a model that includes fluid transport.

These computations serve to demonstrate the sensitivity of wake geometry to modest changes in wing load distribution. (Additional sensitivity studies are detailed in Ref. 3.) In sum, small changes in aircraft configuration and, hence, wing lift distribution can have a profound effect on wake structure. It is an unfortunate fact that techniques giving accurate predictions of load distributions are somewhat lacking, particularly for wings with flaps and slats deployed. However, simple discrete vortex computations can nevertheless be used to assess quickly whether particular lift distributions might result in merging multiple vortex wakes. Whenever vortices of like sign remain in proximity to each other, the merging process must eventually occur. The dynamics of transport and deintensification require the use of

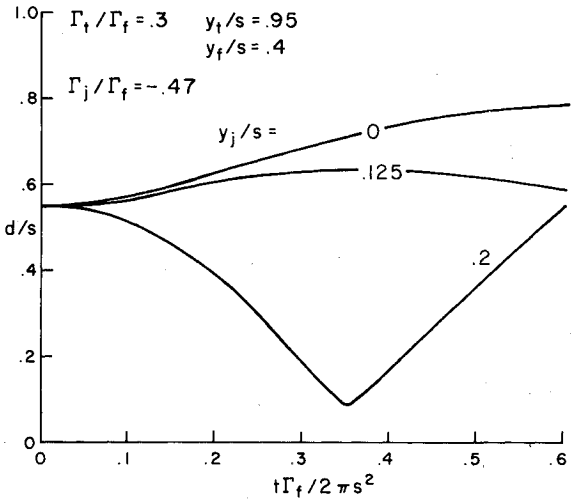

Fig. 6 Sensitivity of the separation distance between tip and flap vortices as a function of the initial position of the fuselage vortex y_j.

a fluid model that includes convective and diffusive processes. In Sec. III, we review a turbulent model under development and highlight the features of a computer code generated to solve the modeled equations of motion.¶

III. Transport Model

Observations of merging[1,7] indicate that the phenomenon can be highly turbulent. Also, any fluid model that attempts to predict the redistribution of vorticity during merging must necessarily include transport. Over the last several years, ARAP has undertaken a detailed modeling study of turbulent flows. This work has led to the refinement of an invariant second-order modeling technique for the Reynolds stress $\langle u_i u_j \rangle$. A comprehensive review of this work and its current status may be found in Lewellen and Teske,[17] along with an examination of the differences between this model and similar models proposed by Lumley and Khajeh-Nouri,[18] Mellor and Yamada,[19] and Wyngaard et al.[20] Evaluation of the modeling constants using simple flow geometries (free jets and wakes,[21] Monin-Obukhov surface layer,[22] flat plate boundary layer) has led to the use of the model in more complicated flows such as free convection,[23] buoyant plumes,[24] and diurnal coastal planetary boundary layers.[25] The extension to aircraft vortices appears a natural one.

The mean equations of motion for neutral flows become

Continuity

$$\frac{\partial U_i}{\partial x_i} = 0 \tag{6}$$

Momentum

$$\frac{\partial U_i}{\partial t} + U_j \frac{\partial U_i}{\partial x_j} = -\frac{\partial \langle u_i u_j \rangle}{\partial x_j} - \frac{1}{\rho}\frac{\partial P}{\partial x_i} + \nu \frac{\partial^2 U_i}{\partial x_j^2} \tag{7}$$

where U_i are cartesian velocities in the x_i direction, t is time, and P is the pressure. The presence of $\langle u_i u_j \rangle$ in Eq. (7) does not permit the system of equations to close without some description of the Reynolds stress. We do this by developing an exact equation for $\langle u_i u_j \rangle$, as shown by Donaldson,[26] and then modeling the necessary third-order correlations and unknown second-order correlations that result in terms of

¶Since submission of the manuscript, Steger and Kutler[37] have described a code capable of making laminar wake merging and decay studies. Their numerical approach differs from ours and their computations do not include turbulent transport.

gradients of $\langle u_i u_j \rangle$, mean flow gradients, and proper scaling and modeling constants. This procedure yields the equations

$$\frac{\partial \langle u_i u_j \rangle}{\partial t} + U_k \frac{\partial \langle u_i u_j \rangle}{\partial x_k} = -\langle u_i u_k \rangle \frac{\partial U_j}{\partial x_k} - \langle u_j u_k \rangle \frac{\partial U_i}{\partial x_k}$$
$$+0.3 \frac{\partial}{\partial x_k}\left(q\Lambda \frac{\partial \langle u_i u_j \rangle}{\partial x_k}\right) - \frac{q}{\Lambda}\left(\langle u_i u_j \rangle - \delta_{ij}\frac{q^2}{3}\right)$$
$$+\nu \frac{\partial^2 \langle u_i u_j \rangle}{\partial x_k^2} - \delta_{ij}\frac{q^3}{12\Lambda} \tag{8}$$

where q^2 is one-half the turbulent kinetic energy ($=\langle u_i u_i \rangle$), and Λ is the turbulent macroscale parameter predicted by the equation

$$\frac{\partial \Lambda}{\partial t} + U_k \frac{\partial \Lambda}{\partial x_k} = 0.35 \frac{\Lambda}{q^2}\langle u_i u_k \rangle \frac{\partial U_i}{\partial x_k} + 0.6q$$
$$+0.3 \frac{\partial}{\partial x_k}\left(q\Lambda \frac{\partial \Lambda}{\partial x_k}\right) - \frac{0.375}{q}\left(\frac{\partial q\Lambda}{\partial x_k}\right)^2 \tag{9}$$

In Eq. (8) time variation and convection are balanced by, respectively, two production terms, turbulent diffusion (with a modeled constant), modeled tendency-toward-isotropy, and modeled isotropic dissipation. In Eq. (9) the time-dependent behavior of the scale and its convection are balanced by turbulent production, dissipation, and two types of diffusion. The constants that appear in these equations have been evaluated by examining simple flows; the resulting values are then consistently and fairly applied without modification to any flow problem of interest.

Equations (7-9) are finite-differenced using a forward-time, centered space scheme on a uniform y-z mesh. These difference equations are then solved using an alternating-direction-implicit (ADI) scheme developed by Peaceman, Rachford and Douglas.[27] The pressure P is obtained from a solution of a Poisson equation

$$\frac{\partial^2 P}{\partial y^2} + \frac{\partial^2 P}{\partial z^2} = -\frac{\partial^2 \langle vv \rangle}{\partial y^2} - 2\frac{\partial^2 \langle vw \rangle}{\partial y \partial z} - \frac{\partial^2 \langle ww \rangle}{\partial z^2}$$
$$+2\frac{\partial V}{\partial y}\frac{\partial W}{\partial z} - 2\frac{\partial V}{\partial z}\frac{\partial W}{\partial y} - \frac{\partial}{\partial t}\left(\frac{\partial V}{\partial y} + \frac{\partial W}{\partial z}\right) \tag{10}$$

using a direct solver developed by Buneman.[28] A discussion of the complete numerical procedure may be found in Teske.[29]

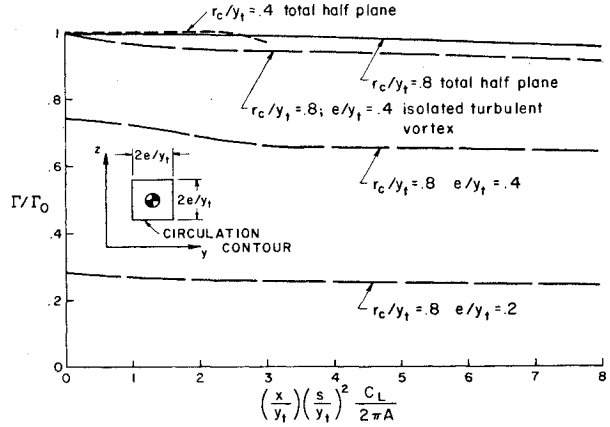

Fig. 7 Decay of circulation in a counter-rotating vortex pair computed about square contours centered at the centroid of vorticity of the half-plane vorticity distribution where Γ_0 is the initial half-plane circulation.

As initial conditions to the merging simulation, we are presently prescribing Gaussians of vorticity (giving their maximum value, center location in the y,z plane, and variance) and isotropic turbulent spots (usually coinciding with the centers of vorticity, with the same decay rate, but with different initial magnitudes) with $\langle u_i u_j \rangle = 0$ for $i \neq j$. Although the program is able to track any consistent set of initial conditions, the use of Gaussians is a convenience and permits a reasonable representation of the initial vortex structure over an adequate number of mesh points to insure time tracking of the merging process.

For boundary conditions we generally set $\langle u_i u_j \rangle = 0$, but cannot set $V = W = 0$ along the boundaries, since every vortex has a far-field decay as r^{-1}. Well outside the region of vorticity, however, the vortex-induced velocities should behave to lowest order as $V \propto z/r^2$ and $W \propto y/r^2$. These expressions provide appropriate boundary conditions for a single vortex but are also just the first terms in a far-field expansion of the moments of the vorticity distribution in the entire computational domain. The stream function ψ, defined from $W = -\partial\psi/\partial y$ and $V = +\partial\psi/\partial z$, is computed from a Poisson equation

$$\frac{\partial^2 \psi}{\partial y^2} + \frac{\partial^2 \psi}{\partial z^2} = -\zeta(y,z,t) = -\left(\frac{\partial W}{\partial y} - \frac{\partial V}{\partial z}\right) \tag{11}$$

dependent on the vorticity ζ at all points (y,z) in the domain. The formal solution to Eq. (11) is

$$\psi(y,z,t) = -\frac{1}{4\pi}\int \omega(y',z',t)\,\ell n[(y-y')^2 + (z-z')^2]\,dy'\,dz' \tag{12}$$

where $\ell n\, r^2$ is the two-dimensional free-space Green's function. If the boundaries are sufficiently far from and completely surround the region containing vorticity, Eq. (12) may be approximated by expanding for $y >> y'$ and $z >> z'$ to obtain

$$\psi(y,z,t) = -\frac{1}{4\pi}\sum_{m=0}^{\infty}\sum_{n=0}^{\infty} I_{mn} G_{mn} \tag{13}$$

where

$$I_{mn} = \int_{-\infty}^{\infty} y'^n z'^m \zeta(y',z',t)\,dy'\,dz' \tag{14}$$

and

$$G_{mn} = \frac{(-1)^{m+n}}{m!n!}\frac{\partial^{m+n}}{\partial z^m \partial y^n}(\ell n\, r^2) \tag{15}$$

From ψ we obtain V and W, and use these values along the boundary of our computational domain. Our work suggests that $(m+n)$ need be no larger than 2 for most applications.

IV. Vortex Transport Computations

The transport code has been used to investigate several vortex wake problems of interest. Flowfields that are to be simulated must necessarily lend themselves to a parabolic approximation in one direction. The downstream direction of a vortex wake is observed under most cases to be sufficiently slowly varying to justify a parabolic approximation in this direction. However, the flow in the immediate vicinity of a lifting body, where regions of separation can exist, cannot be simulated at this time. The transport code in this case must be applied downstream of these regions. Several computations demonstrating the flexibility and predictive capability of the code are now given.

Decay of a Vortex Pair

The simplest vortex wake is generated by an aircraft in cruise configuration. The resulting wake may be described by

a simple vortex pair whose vorticity distributions are centered at $(\pm y_t, 0)$ with maxima $\pm \pi r_c^2 \zeta/\Gamma = 1$ and variance r_c; that is

$$\frac{\pi r_c^2 \zeta}{\Gamma} = \exp\left[-\frac{(y-y_t)^2+z^2}{r_c^2}\right] - \exp\left[\frac{(y+y_t)^2+z^2}{r_c^2}\right] \quad (16)$$

The turbulent energy is taken to be Gaussians of magnitude $(2\pi y_t q/\Gamma)^2 = 0.3$. We make two computations with the viscous core radius $r_c/y_t = 0.4$ and 0.8 and the scale $\Lambda/y_t = 0.2$. These calculations were carried out in time and then transformed to downstream distance through $x = U_\infty t$.

Figure 7 shows the decay of circulation as a function of distance behind the aircraft. For the case with the initially tight vortices ($r_c/y_t = 0.4$), a downstream interval exists over which the total half-plane circulation remains constant. This interval has been discussed with the aid of Fig. 1 and is the time required to diffuse the vorticity to the wake centerline. Note that the initially dispersed vortices ($r_c/y_t = 0.8$) show an immediate reduction in their half-plane circulation. Shown also in Fig. 7 is the decay of circulation about a square contour of side $2e/y_t$ centered on the centroid of vorticity. For comparison, the computation for the initially dispersed vortices ($r_c/y_t = 0.8$) was run with an infinite separation between vortices. The circulation decay of this isolated vortex decays less rapidly than does the pair, with the maximum turbulence level occurring in the pair approximately twice that in the isolated vortex. At $(x/y_t)(s/y_t)^2 C_L/2\pi A = 8$, the vortex circulation has decayed no more than 0.86 of its initial value. For a B-747 with a rectangularly loaded wing and $C_L \sim 1$, the total downstream distance traveled is about 10 km. The vortex pair does not promote the production of turbulence, and hence ages quite slowly.

Instantaneous streamlines at the beginning and end of the computation with $r_c/y_t = 0.8$ are shown in Fig. 8. Here the coordinate system is one in which the fluid at infinity is at rest; therefore, the pair descends downward, but with very little change in its overall character. Its downwash velocity attenuates slightly from its initial value.

Decay of a Vortex Pair in a Turbulent Bath

To illustrate the role of atmospheric turbulence on the decay of a vortex pair, we make two computations in which the vortices are immersed in a constant $\epsilon = 0.125 q^3/\Lambda$ background. The turbulence is maintained by a uniform axial shear $U = \beta z$ with the turbulent scale specified as $\Lambda/y_t = 0.2$ and 2.0, and the turbulence determined by an application of Donaldson's superequilibrium theory.[26] The corresponding turbulent kinetic energies are taken as $(2\pi y_t q/\Gamma)^2 = 0.025$ and 0.116, respectively, so that $\epsilon^{1/3} = 2$ cm$^{2/3}$/sec as suggested by Tombach[30] for light and light-to-moderate turbulence. These turbulent kinetic energy levels can be achieved in a stable atmosphere. The variance is taken as $r_c/y_t = 0.5$ with the vortices centered at $y/y_t = \pm 1$.

Figure 9 shows the circulation decay computed about a box contour of side $2e/y_t$ centered at the centroid of the vorticity. At the end of the computation (typically a wake age of 4 min), levels of various box sizes differ in the two runs by a factor of 4. These results emphasize the importance of scale and caution against too simple a parameterization of the atmosphere. They also show that significant decay of circulation occurs in a turbulent atmosphere, while the quiescent atmosphere of Fig. 7 produces very little decay over comparable time scales. The ability of the atmosphere to control the ultimate fate of a vortex wake is evident even for relatively low turbulence levels. We liken the turbulent atmosphere to an infinite reservoir of turbulent kinetic energy which can, over unlimited time, nibble away at the vortex wake.

Vortex Merging

An isolated vortex has streamlines that are circles centered on the vortex axes. Diffusion is the only mechanism that can redistribute vorticity radially outward and, even then, aging of a vortex is extremely slow. The axisymmetric vortex is quite stable, sustaining low turbulence levels and, in fact, damping turbulence in its central region (the viscous core). It is just in this region where vorticity is a maximum, with the only turbulent redistribution of vorticity resulting from turbulence diffused into the core. Observations[31] show that vortex cores from simply loaded wings are nearly laminar; our computations[6] using second-order closure modeling confirm this feature.

The presence of two or more vortices in proximity destroys the axial symmetry of a vortex by adding an induced straining field. Once the symmetry has been destroyed, turbulence can be produced, leading to subsequent diffusion of vorticity. As a first calculation of the merging phenomenon itself, we examine the merging between two like-sign, equal strength vortices. Two Gaussians of vorticity $\pi d^2 \zeta/2\Gamma = 1$ with variance $r_c = 0.35d$ are placed at $y = \pm d/2$, $z = 0$, along with spots of turbulent kinetic energy of magnitude

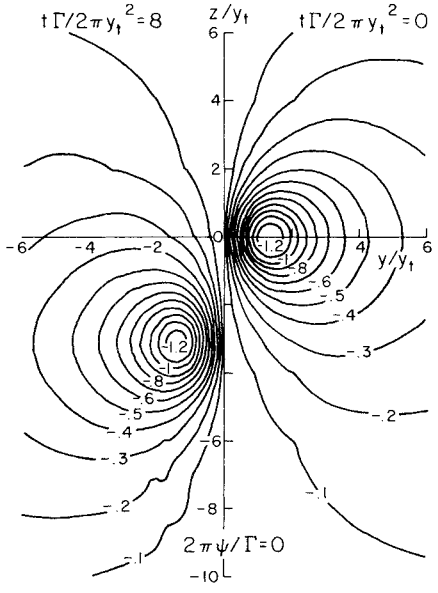

Fig. 8 Instantaneous streamlines at $t\Gamma/2\pi y_t^2 = 0$ and 8. Streamlines for $t\Gamma/2\pi y_t^2 = 8$ have been reflected across the z axis.

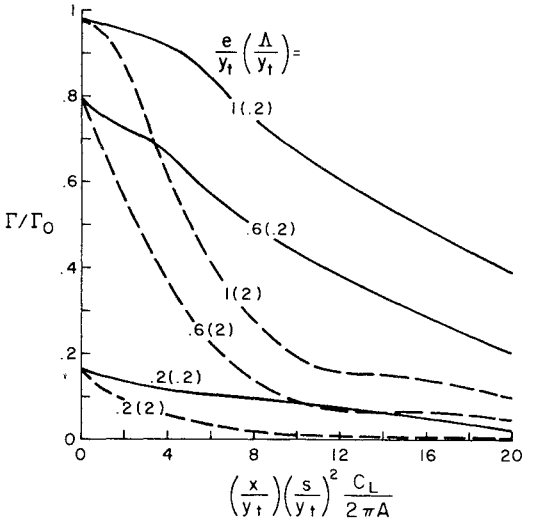

Fig. 9 Decay of circulation in a counter-rotating vortex pair immersed in a turbulent atmosphere with constant dissipation rate $\epsilon^{1/3} = 2$ cm$^{2/3}$/sec for contour box sizes e and background turbulent macroscale length Λ. Γ_0 is the initial half-plane circulation.

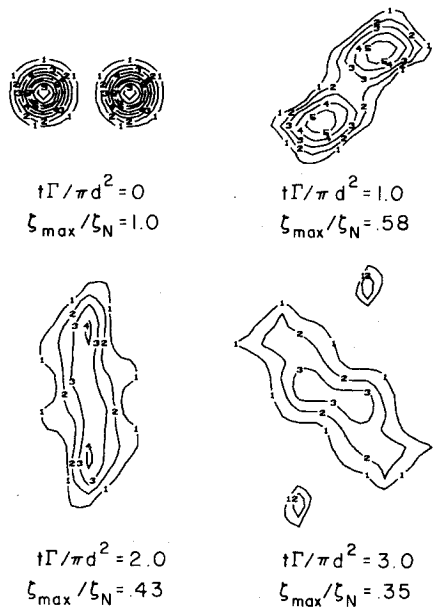

Fig. 10 Mean vorticity distribution during the merging of two like-sign, equal-strength vortices $2\zeta_N\Gamma/\pi d^2 = 8.0$. Contour numbers indicate tenths of normalized value; i.e., 1 equals $0.1\zeta_N$ contour level, $2 = 0.2\zeta_N$ level, etc.

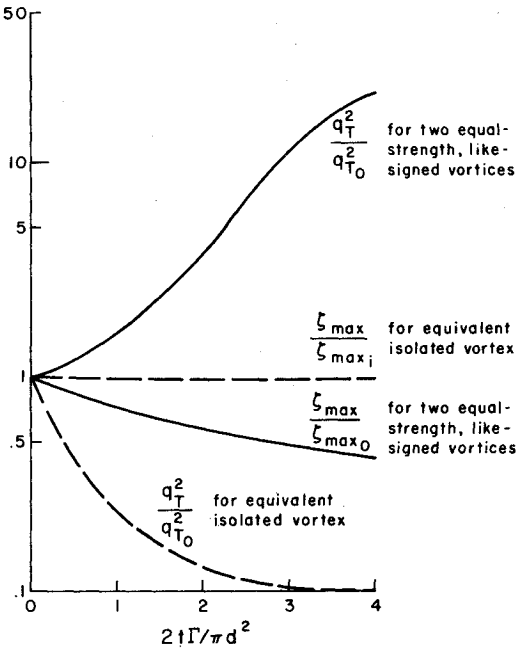

Fig. 12 Comparison of the total turbulent kinetic energy and maximum vorticity as a function of time between an isolated axisymmetric vortex and two like-sign, equal-strength vortices. Here, $q_T^2/q_{T_0}^2 = \int q^2 dA / \int q^2 dA|_{t=0}$ and $\zeta_{\max i}/\zeta_{\max 0} = 0.4$.

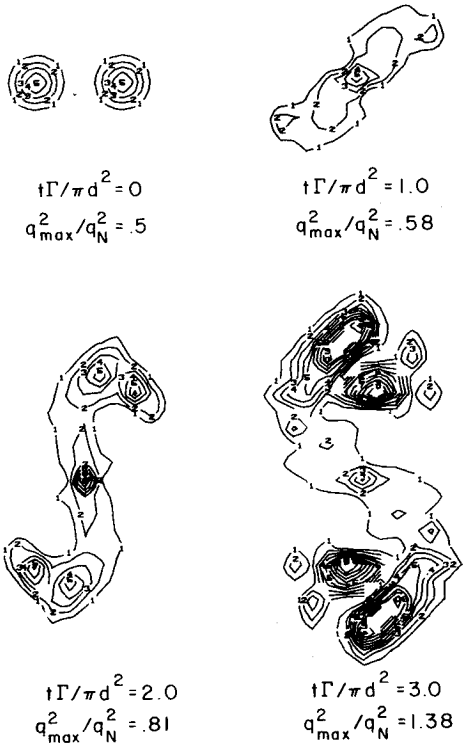

Fig. 11 Twice the turbulent kinetic energy distribution during the merging of two like-sign, equal-strength vortices. $(q_N\pi d/\Gamma)^2 = 0.02$. Contour numbers indicate tenths of normalized q_N^2 value.

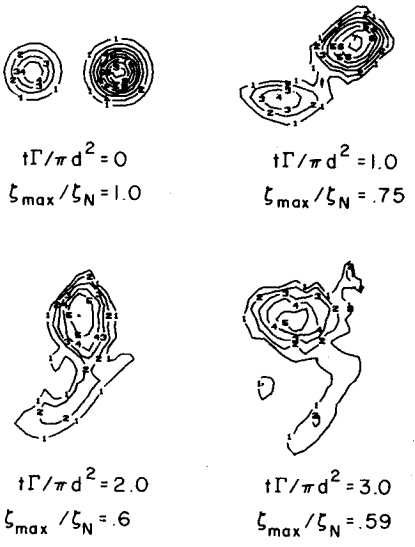

Fig. 13 Mean vorticity distribution during the merging of two like-sign vortices. The vortex on the left is one-half the strength of the vortex on the right. $2\zeta_N\Gamma/\pi d^2 = 8.0$. Isopleth labeling notation as in Fig. 10.

$(\pi dq/\Gamma)^2 = 0.01$. The integral scale parameter is initially taken $\Lambda = 0.1d$.

The results of this computation are shown in Figs. 10 and 11 where instantaneous distributions of vorticity and turbulent kinetic energy are shown in isopleth form. The counterclock wise rotation of the pair is as expected. It is interesting to note that the vorticity takes on a discernibly more axisymmetric structure at $t\Gamma/\pi d^2 = 3$ than does the turbulent kinetic energy. The initial redistribution of vorticity is governed by convection, while the time scale for turbulent redistribution through diffusion is the order of $\Lambda/q \sim 1$, showing that sufficient time has not yet elapsed for the turbulent quantities to equilibrate.

We may compare these results with an equivalent isolated vortex decay computation to illustrate the significance of the merging phenomenon in terms of aging of the vortex flowfield. For this we compute the decay of an isolated axisymmetric vortex whose circulation equals that of the pair. The core radius r_c is chosen to make the polar moment of the vorticity distribution computed about the centroid equal to that of the merging pair. The initial turbulence distribution is taken to be twice the magnitude of the pair so that the initial total turbulent kinetic energies in both computations are equal. The integral scale parameter Λ is again taken to be $0.1d$. The calculations were made with an axisymmetric code developed by Sullivan.[32]

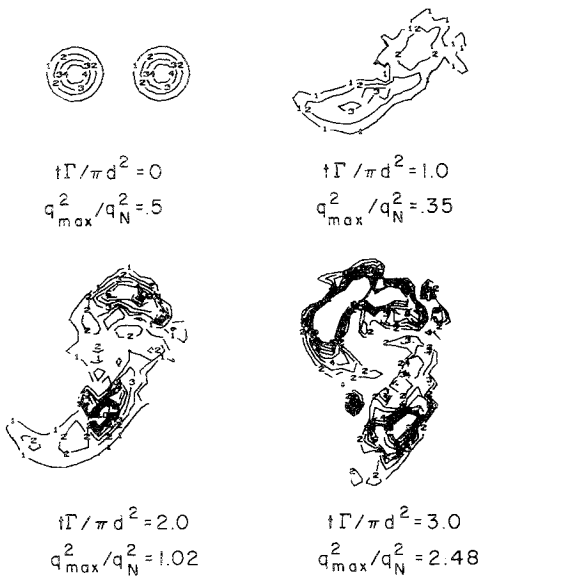

Fig. 14 Twice the turbulent kinetic energy distribution during the merging of two like-sign vortices. The vortex on the left is one-half the strength of the vortex on the right. $(q_N \pi d/\Gamma)^2 = 0.02$ with notation in Fig. 11.

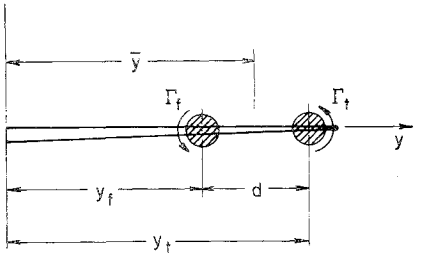

Fig. 15 Illustration of the relative positions and strengths of two like-sign vortices behind a wing.

Figure 12 shows the behavior of the total turbulent kinetic energy and vorticity in the crossplane as a function of time for the two cases. The turbulence level supported by the axisymmetric isolated vortex is far less than initially introduced, while the breakdown of the axisymmetric structure about each vortex in the merging pair results in the production of turbulent kinetic energy and Reynolds stress. The mean vorticity diffuses outward in addition to spreading convectively. The production of turbulence is the transport mechanism that diffuses vorticity to the wake centerline and results in the decay of circulation in the wake, as shown schematically in Fig. 1.

We have made calculations involving merging of unequal strength vortices with the second vortex 50%, 20%, and −20% the strength of the first vortex and with all other initial conditions equal to those used in the merging calculation of two like-sign, equal-strength vortices. Comparison between merging of equal-sign and strength vortices and merging with the second vortex 50% of the strength of the first may be made by comparing Figs. 10 and 11 with Figs. 13 and 14. Merging of equal-strength vortices involves equal redistribution of both vortices, while the 50% vortex in the unequal merging computation is convected about the stronger vortex. The structure of the stronger vortex is unaltered during this process. While the merging of the unequal strength vortices produces a higher local level of turbulent kinetic energy (most notably at $t\Gamma/\pi d^2 = 3$), the spread of the turbulent kinetic energy is greater in the like-sign, equal-strength computation. The results for merging of the 20% and −20% strength second vortices are qualitatively the same as observed for the 50% unequal computation. The weaker vortex convects around the stronger vortex with very little change in the structure of the stronger vortex.

A Minimum Hazard Vortex Wake

The results given previously may now be used to infer a minimum hazard aircraft wake condition. For this we neglect the effect of the opposite merging pair on the other wing, since the first-order effect of the vortices from the opposite wing brings about wake descent. If a vortex were sufficiently close to the aircraft centerline, its mate would indeed dominate it. Here, however, we are interested in merging and are looking for a configuration wherein the two vortex pairs remain together. A schematic representation of the initial wake is shown in Fig. 15.

If lift is held constant in evaluating the hazard between various merging wakes, then

$$L = \rho U_\infty 2\bar{y}(\Gamma_f + \Gamma_t) \tag{17}$$

with the centroid of the system given by

$$\bar{y} = \frac{y_f \Gamma_f + y_t \Gamma_t}{\Gamma_f + \Gamma_t} \tag{18}$$

Vortex hazard is evaluated at NASA[33,34] by measuring the rolling moment induced on a following wing by the vortex wake. Although the calculation of aerodynamic loads on a wing using strip theory is of limited value even in uniform flow, it is adequate if only trends and minima are to be obtained. The torque induced on a constant chord airfoil is

$$T = \frac{1}{2}\rho U_\infty^2 \int_{-s_f}^{s_f} c_{\ell_\alpha} \frac{W}{U_\infty} c_f y \, dy \tag{19}$$

where the subscript f denotes the follower aircraft. Substituting Eqs. (17) and (18) into Eq. (19), we obtain an equation for the maximum rolling moment

$$C_\ell = \frac{c_{\ell_\alpha} C_L}{16\pi} \frac{ds^2 I}{s_f^2 s[(1 - d/s) + I]} \tag{20}$$

with

$$I = \frac{4\pi}{\Gamma_t d} \int_{-2s_f/d}^{2s_f/d} Wy \, dy \tag{21}$$

The decay of the maximum rolling moment encountered as a function of downstream distance for the case where the wing span of the follower aircraft is 20% of the wing span of the generator (typical of a Learjet behind a B-747) is shown in Fig. 16. The first observation apparent from the figure is that the rolling moment is a minimum when the merging vortices are of equal strength. Selection of the critical spacing d/s is not as easy, with $d/s = 0.6$ and 0.8 comparing quite closely. However, the $d/s = 0.6$ spacing shows a slight advantage. If we refer to Fig. 2 (our wake classification chart), the d/s beyond which equal-strength vortex pairs separate is about 0.8, so that the equal strength with separation $d/s = 0.6$ is a minimum hazard wake for a follower aircraft with a span 20% of the span of the generating aircraft.

The oscillations occurring in the rolling moment as a function of downstream distance are expected and are associated with the orientation of the unmerged distributions of vorticity relative to the follower aircraft. As the merging process moves to completion, the amplitude of the oscillations decay, with the average value of rolling moment (averaged between peaks and troughs) decaying smoothly. For a follower aircraft with a span 60% of the span of the generator, our computations show that equal-strength merging again results in a minimum induced rolling moment

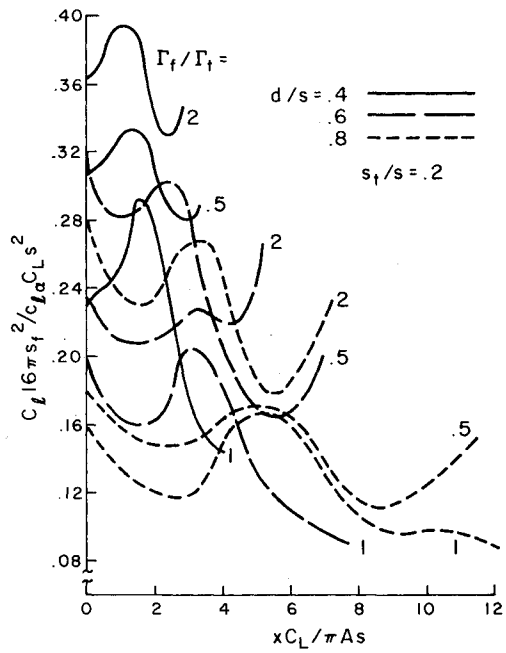

Fig. 16 Decay of the maximum rolling moment encountered by a follower aircraft of semispan 20% of the semispan of the generating aircraft for three values of d/s and three ratios of Γ_f/Γ_t.

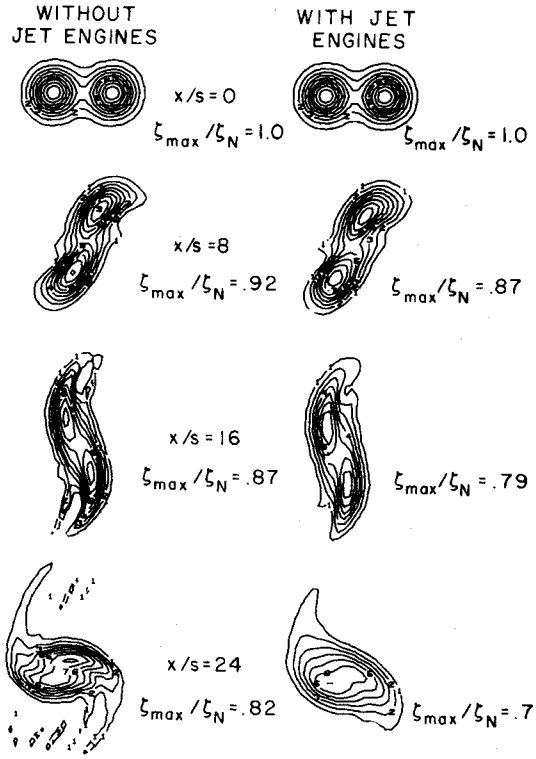

Fig. 17 Contour plots of the trailed vorticity ζ within simulated aircraft wakes. $\zeta_N = 48.5\Gamma/2\pi s^2$.

near a $d/s = 0.6$, although the difference in level between various relative vortex strengths is not as significant as for the smaller follower aircraft.

These results indicate that a minimum hazard wake for a small follower aircraft is achieved by having equal-strength flap and tip vortices, with the tip vortices located at $y = \pm s$ and the flap vortices located at $y = \pm 0.4s$. Experimental verification of this finding is forthcoming.

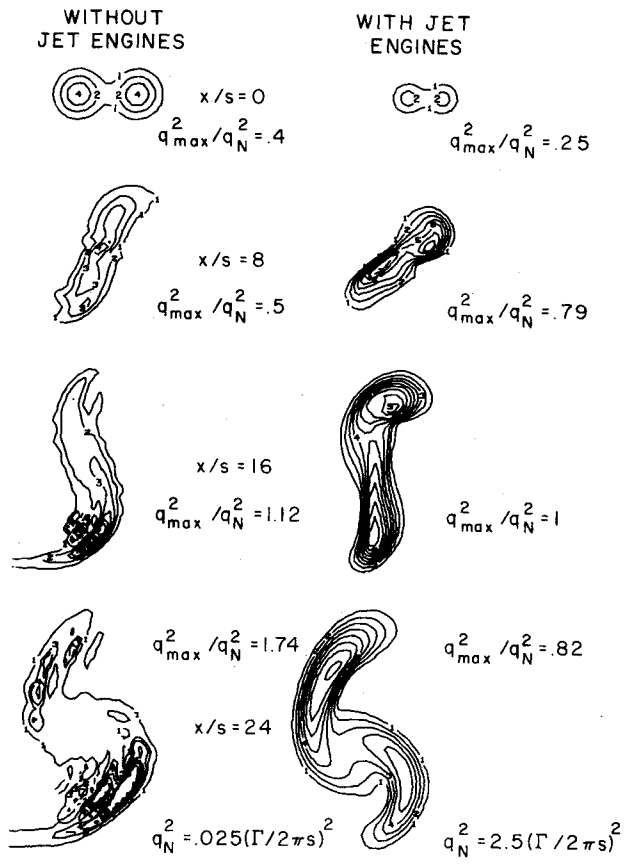

Fig. 18 Contour plots of twice the turbulent kinetic energy q^2 within simulated aircraft wakes. The normalizing q_N^2 is different for the two cases shown.

Merging in Aircraft Wakes

To illustrate typical merging in aircraft wakes, we conclude our model calculations by presenting the results of two computations. In both cases the tip and flap vortices are of like sign and equal strength, positioned at $y = \pm 0.95s$ and $y = \pm 0.4s$, respectively. The vortices are of strength $2\pi s^2\zeta/\Gamma = 1$ with $r_c = 0.2s$. Turbulence is centered on the vortices with strengths $(2\pi sq/\Gamma)^2 = 0.01$, and $\Lambda = 0.2s$ initially. Our second calculation adds cold-engine exhaust of magnitude $\pi s\Delta U/\Gamma = 8$ and variance $r_c = 0.14s$ positioned at $y = \pm 0.75s$ and $\pm 0.4s$, $z = 0.08s$, in simulation of the approximate locations of the engine exhausts of a B-747 aircraft. Additional turbulence of magnitude $(2\pi sq/\Gamma)^2 = 0.64$ are added to simulate the expected turbulence produced by the exhausts. The flight speed of the aircraft is $U_\infty = 40.0\Gamma/2\pi s$.

Full-scale flight tests have observed that engine thrust levels make a measurable change in the decay rate of a vortex wake.[35] The basic merging phenomenon will probably not be altered by the presence of the jet exhausts (even with the flap vortex located directly over an engine), but the additional jet turbulence should result in additional turbulent diffusion of the trailed vorticity. Our results for vorticity, turbulent kinetic energy, and axial velocity excess are presented in Figs. 17-19 in isopleth form normalized by an overall maximum except in the turbulent energy case where significantly larger values of turbulence exist behind the engine exhausts. The vorticity plots (Fig. 17) show that the presence of jet engines does not hinder the merging of the tip and flap vortices. At 12 spans downstream, the jet engines give slightly more spreading of the trailed vorticity and lead to a slightly lower maximum vorticity value. The merging continues in the presence of the elevated turbulence in the jet exhausts shown in Fig. 18.

It is likely that appreciable redistribution of trailed vorticity is yet to occur owing to the large values of turbulent kinetic

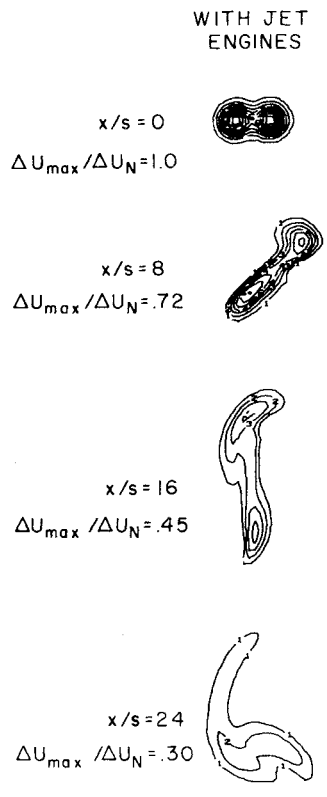

Fig. 19 Contour plots of the jet exhaust axial velocity excess ΔU within a simulated aircraft wake. $\Delta U_N = 8.0\Gamma/2\pi s$.

energy still left in the wake. This feature is overemphasized by taking the initial integral scale parameter Λ/s to be 0.2 when it should probably be initialized somewhat smaller.

Jet exhaust axial velocity excess contour plots are shown in Fig. 19. The inboard engine exhaust introduced into the flap vortex is slower to decay than the exhaust from the outboard engine, demonstrating the suppression of the production of turbulence by swirl. Engine exhausts are not the same temperature as the surrounding fluid, but these effects are yet to be investigated. Further vortex wake calculations may be found in Bilanin et al.[3]

V. Conclusions

Several conclusions from this study can be made with regard to predicting aircraft vortex wake strength and structure.

1) The number, strengths, and initial positions of vortices trailed from an aircraft wing are determined by the detailed lift distribution on the wing. Prior to this study, only inviscid models were available to predict the swirl velocity distributions in each vortex and the interactions between vortices. The vortex-vortex interaction, called merging, which has been shown in the laboratory, in flight tests, and through analytic techniques to lead to rapid aging of a wake involves convection and turbulent diffusion of trailed vorticity. A transport model is now available to predict viscous wake interactions.

2) Calculations using this vortex wake transport code have shown that a minimum hazard wake is trailed from a generating aircraft when the aircraft configuration is such that a flap and wing tip vortex of the same sign and strength are shed from each wing. To achieve this optimum, the flap vortex is located outboard approximately 40% of the distance to the tip vortex. The vortices merge, during which convection and diffusion distribute the trailed vorticity widely over the wake.

3) The effect of ambient atmospheric turbulence on the aging of an aircraft wake was investigated at constant turbulent dissipation rate. It was shown that under stable atmospheric conditions, when the atmospheric macroscale may be less than or equal to the vortex spacing, misleading results may be obtained if vortex aging is correlated only with the turbulent dissipation rate. This result cautions against using one parameter to characterize the ability of the atmosphere to dissipate aircraft wake vortices.

4) Calculations using the transport code show that engine exhausts do not appreciably alter the merging phenomenon. Results suggest that the turbulence added to the wake by engine exhausts help further to diffuse the trailed vorticity prior to, during, and after vortex merging has occurred.

5) Comparison of the turbulence produced during the merging of equal-strength, like-sign vortices with an equivalent isolated vortex shows clearly the importance of turbulent transport during the merging phenomenon.

Acknowledgment

This work was sponsored by the National Aeronautics and Space Administration, Langley Research Center, under Contract NAS1-13932, and by the Air Force Flight Dynamics Laboratory under Contract F33615-73-C-3138.

References

[1] Dunham, R. E., Jr., "Model Tests of Various Vortex Dissipation Techniques in a Water Towing Tank," NASA LWP-1146, Jan. 1974.

[2] Corsiglia, V. R. and Dunham, R. E., Jr., "Aircraft Wake-Vortex Minimization by Use of Flaps," *Proceedings NASA Symposium on Wake Vortex Minimization*, Wash. D. C., Feb. 25-26, 1976, pp. 303-336.

[3] Bilanin, A. J., Teske, M. E., Donaldson, C. duP, and Snedeker, R. S., "Viscous Effects in Aircraft Trailing Vortices," *Proceedings NASA Symposium on Wake Vortex Minimization*, Wash., D. C., Feb. 25-26, 1976, pp. 55-122.

[4] Bilanin, A. J., Snedeker, R. S., and Teske, M. E., "Interaction and Merging of Line Vortices," Aeronautical Research Associates of Princeton, Inc., Princeton, N. J., Tech. Memo. No. 76-5, June 1976, (submitted for publication *Journal of Fluid Mechanics*).

[5] Rossow, Vernon J., "Inviscid Modeling of Aircraft Trailing Vortices," *Proceedings NASA Symposium on Wake Vortex Minimization*, Wash., D. C., Feb. 25-26, 1976, pp. 4-54.

[6] Donaldson, C. duP. and Bilanin, A. J., "Vortex Wakes of Conventional Aircraft," AGARDograph No. 204, May 1975.

[7] Ciffone, D. L. and Lonzo, C., Jr., "Flow Visualization of Vortex Interactions in Multiple Vortex Wakes Behind Aircraft," NASA TM X-62, 459, June 1975.

[8] Donaldson, C. duP., Snedeker, R. S., and Sullivan, R. D., "A Method of Calculating Aircraft Wake Velocity Profiles and Comparison with Full-Scale Experimental Measurements," *Journal of Aircraft*, Vol. 11, Sept. 1974, pp. 547-555.

[9] Betz, A., "Behavior of Vortex Systems," NACA TM 713, June 1933, (trans. from *ZAMM*, Vol. XII.3, June 1932).

[10] Bilanin, A. J., Donaldson, C. duP., and Snedeker, R. S., "An Analytic and Experimental Investigation of the Wakes Behind Flapped and Unflapped Wings," AFFDL-TR-74-90, Air Force Flight Dynamics Lab., Wright-Patterson AFB, Ohio, May 1974.

[11] Fink, P. T. and Soh, W. K., "Calculation of Vortex Sheets in Unsteady Flow and Applications in Ship Hydrodynamics," School of Mech. and Ind. Engr., The University of New South Wales, Australia, Rept. NAV/ARCH 74/1, April 1974.

[12] Moore, D. W., "Numerical Study of the Roll-Up of a Finite Vortex Sheet," *Journal of Fluid Mechanics*, Vol. 63, No. 2, April 1974, pp. 225-235.

[13] Chorin, A. J. and Bernard, P. S., "Discretization of a Vortex Sheet, with an Example of Roll-Up," *Journal of Computational Physics*, Vol. 13, Nov. 1973, pp. 423-429.

[14] Hackett, J. E. and Evans, M. R., "Vortex Wakes Behind High Lift Wings," *Journal of Aircraft*, Vol. 8, May 1971, pp. 334-340.

[15] Yates, J. E., "Calculation of Initial Vortex Roll-Up in Aircraft Wakes," *Journal of Aircraft*, Vol. 11, July 1974, pp. 397-400.

[16] Lin, C. C., *On the Motion of Vortices in Two Dimensions*, University of Toronto Press, Toronto, 1943.

[17] Lewellen, W. S. and Teske, M. E., "Turbulence Modeling and Its Application to Atmospheric Diffusion," EPA-600/4-75-016, Environmental Protection Agency, Raleigh, N.C., Dec. 1975.

[18] Lumley, J. L. and Khajeh-Nouri, B., "Computational Modeling of Turbulent Transport," *Advances in Geophysics, 18A*, Academic Press, N.Y., 1974, pp. 169-192.

[19]Mellor, G. L. and Yamada, T., "A Hierarchy of Turbulence Closure Models for Planetary Boundary Layers," *Journal of Atmospheric Sciences*, Vol. 31, Oct. 1974, pp. 1791-1806.

[20]Wyngaard, J. C., Cote, O. R., and Rao, K. S., "Modeling the Atmospheric Layer," *Advances in Geophysics, 18A*, Academic Press, N.Y., 1974, pp. 193-212.

[21]Lewellen, W. S., Teske, M. E., and Donaldson, C. duP., "Application of Turbulent Model Equations to Axisymmetric Wakes," *AIAA Journal*, Vol. 12, May 1974, pp. 620-625.

[22]Lewellen, W. S. and Teske, M. E., "Prediction of the Monin-Obukhov Similarity Functions from an Invariant Model of Turbulence," *Journal of Atmospheric Sciences*, Vol. 30, Oct. 1973, pp. 1340-1345.

[23]Lewellen, W. S., Teske, M. E., and Donaldson, C. duP., "Variable Density Flows Computed by a Second-Order Closure Description of Turbulence," *AIAA Journal*, Vol. 14, March 1976, pp. 382-387.

[24]Teske, M. E. and Lewellen, W. S., "Example Calculations of Atmospheric Dispersion Using Second-Order Closure Modeling," Presented Third Symposium on Atmospheric Turbulence, Oct. 19-22, 1976, Raleigh, N.C.

[25]Lewellen, W. S. and Teske, M. E., "A Second-Order Closure Model of Turbulent Transport in the Coastal Planetary Boundary Layer," Presented National Conference on Coastal Meteorology, Sept. 21-23, 1976, Virginia Beach, Va.

[26]Donaldson, C. duP., "Atmospheric Turbulence and the Dispersal of Atmospheric Pollutants," *AMS Workshop on Micrometeorology* (D. A. Haugen, ed.), Science Press, pp. 313-390.

[27]Carnahan, B., Luther, H. A., and Wilkes, J. O., *Applied Numerical Methods*, Wiley, N.Y., 1969, pp. 452-453, 508.

[28]Buneman, O., "A Compact Non-Iterative Poisson Solver," SUIPR Rept. No. 294, Inst. for Plasma Research, Stanford Univ., Stanford Calif., May 1969.

[29]Teske, M. E., "Vortex Interactions and Decay in Aircraft Wakes," Part II: "The Vortex Wake Computer Program User Manual." Part III: "The Vortex Wake Computer Program Programmer Manual," ARAP Rept. 271, Aeronautical Research Associates of Princeton, Inc., Princeton, N. J., March 1976.

[30]Tombach, I., "Observations of Atmospheric Effects of Vortex Wake Behavior," *Journal of Aircraft*, Vol. 10, Nov. 1973, pp. 641-647.

[31]Bradshaw, P., "The Effects of Streamline Curvature on Turbulent Flow," AGARDograph 169, Aug. 1973.

[32]Sullivan, R. D., "A Program to Compute the Behavior of a Three-Dimensional Turbulent Vortex," ARL-TR-74-0009, Dec. 1973.

[33]Croom, D. R., "Development of the Use of Spoilers as Vortex Attenuators," *Proceedings NASA Symposium on Wake Vortex Minimization*, Wash., D. C., Feb. 25-26, 1976, pp. 337-370.

[34]Stickle, Joseph W., and Kelly, Mark W., "Ground Based Facilities for Evaluating Vortex Minimization Concepts," *Proceedings NASA Symposium on Wake Vortex Minimization*, Wash., D.C., Feb. 25-26, 1976, pp. 123-154.

[35]Smith, H. J., "A Flight Test Investigation of the Rolling Moments Induced on a T 37B Airplane in the Wake of a B-747 Airplane," NASA TM X-56,031, April 1975.

[36]Rossow, V. J., "Convective Merging of Vortex Cores in Lift-Generated Wakes," AIAA Paper 76-415, San Diego, Calif., July 1976.

[37]Steger, J.L. and Kutler, P., "Implicit Finite-Difference Procedures for the Computation of Vortex Wakes," AIAA Paper 76-385, San Diego, Calif., July 1976.